Thermal Design of the Sample Handling Assembly in the Sampling and Caching Subsystem on the Mars 2020 Rover

Keith S. Novak[1], Jason G. Kempenaar[2], Matthew Redmond[3], Takuro Daimaru[4]
NASA Jet Propulsion Laboratory, California Institute of Technology, Pasadena, CA, 91109

and

Chern-Jiin Lee[5]
Applied Sciences Laboratory, Inc., Baldwin Park, CA 91706

The Mars 2020 Rover is scheduled to land on Mars on February 18, 2021. One of the primary mission objectives for the Mars 2020 Rover is to collect a set of Martian regolith samples for potential future return to Earth. Regolith and rock samples will be collected and placed into sample tubes using a coring drill, located at the end of a large Robotic Arm, on the outside of the rover. Filled sample tubes will be transferred from the outside of the Rover into the Adaptive Caching Assembly (ACA), located inside the Rover chassis, via the Bit Carousel. Once the filled sample tube is brought into the ACA, the Sample Handling Assembly (SHA) will transfer it to all of the internal processing stations of the ACA for volume assessment, sealing and finally drop-off on the Martian surface. The ACA is a volume within the rover chassis that is not temperature-controlled. Actuators inside the SHA and its End Effector (EE) must be warmed to above -55°C and -25°C, respectively, prior to use. This paper discusses the thermal design of the SHA that uses heaters and temperature sensors to warm up and maintain the temperature-sensitive arm components within temperature limits during operation. Thermal performance predictions for Mars surface operations are also presented.

Nomenclature

ACA	=	Adaptive Caching Assembly
AFT	=	Allowable Flight Temperature
CCMD	=	Caching Component Mounting Deck
DC	=	Duty Cycle
DTE	=	Direct-to-Earth
DP	=	Design Principle
EDL	=	Entry, Descent and Landing
EE	=	End Effector
ELB	=	Elbow Actuator
ENDS	=	End Effector Housing
gDRT	=	Gas Dust Removal Tool
HGA	=	High Gain Antenna

[1] Principal Engineer, Spacecraft Thermal Engineering Group, Jet Propulsion Laboratory, 4800 Oak Grove Drive, M/S 125-123, Pasadena, CA 91109.
[2] Systems Engineer, Instrument and Payload Thermal Engineering Group, Jet Propulsion Laboratory, 4800 Oak Grove Drive, M/S 125-123, Pasadena, CA 91109.
[3] Thermal Engineer, Instrument and Payload Thermal Engineering Group, Jet Propulsion Laboratory, 4800 Oak Grove Drive, M/S 125-123, Pasadena, CA 91109.
[4] Thermal Engineer, Thermal Fluid Systems and Mission Operations Group, Jet Propulsion Laboratory, 4800 Oak Grove Drive, M/S 125-123, Pasadena, CA 91109.
[5] Senior Engineer, Applied Sciences Laboratory, Inc., 13111 Brooks Drive, Suite A & B, Baldwin Park, CA 91706.

Copyright © 2019 California Institute of Technology. Government sponsorship acknowledged.

HS	=	Housing
JPL	=	Jet Propulsion Laboratory
LN	=	Linear Stage
LO TG HS	=	Lower Tube Gripper Housing
Ls	=	Solar Longitude
LTST	=	Local True Solar Time
Mastcam-Z	=	Mast Camera with Zoom feature
MarsWRF	=	Mars Weather Research and Forecasting Model
MAX	=	Maximum
MECH	=	Mechanism
MIN	=	Minimum
MMRTG	=	Multi-Mission Radioisotope Thermoelectric Generator
MSL	=	Mars Science Laboratory
NASA	=	National Aeronautics and Space Administration
OP	=	Operating
PIXL	=	Planetary Instrument for X-ray Lithochemistry
PRT	=	Platinum Resistance Thermometer
RA	=	Robotic Arm
RLGA	=	Rover Low Gain Antenna
RPFA	=	Rover Pyro Firing Assembly
RSM	=	Remote Sensing Mast
RUHF	=	Rover Ultra-High Frequency
SCS	=	Sampling and Caching Subsystem
SHA	=	Sample Handling Assembly
SHERLOC	=	Scanning Habitable Environments with Raman & Luminescence for Organics and Chemicals
SHD	=	Shoulder
SuperCam	=	Science Instrument at top of RSM Mast
Tau	=	Optical Depth of the Atmosphere
TD	=	Thermal Desktop®
UHF	=	Ultra High Frequency
WCC	=	Worst-Case Cold
WCH	=	Worst-Case Hot

I. Introduction

NASA is scheduled to launch the Mars 2020 Rover to Mars in July of 2020. After a seven-month cruise, the Mars 2020 Rover will touch down on the surface of Mars on February 18, 2021. The Mars 2020 Rover will land in Jezero Crater (at 18.5°N latitude), where it will investigate the geology of the site, assess the habitability of the site and look for signs of ancient Martian life. One of the primary science objectives of this Rover mission is to extract and cache a collection of soil and rock samples from the surface of Mars for potential return to Earth by a future mission. The Mars 2020 Rover design is heavily derived from the Mars Science Laboratory (MSL) Rover design. Many of the changes that were made to the MSL Rover design for Mars 2020 were driven by accommodation of the seven science instruments and the Sampling and Caching Subsystem (SCS). A full description of the preliminary thermal design of the Mars 2020 Rover, including a description of its science instruments, has been previously published.[1] A later paper describes the detailed surface thermal design of the Mars 2020 Rover.[2]

When the Mars 2020 Rover is fully deployed on Mars, it will have a wheelbase of 2.8 m long and 2.3 m wide, and a ground clearance of more than 40 cm (with the stowed Mars helicopter attached to the belly pan). Engineering hardware, located on the outside of the Rover, is shown in Figure 1. There are many heritage hardware elements from MSL that will be re-used on Mars 2020. Some of these are exact copies of MSL designs; others are MSL build-to-print designs with slight modifications. The Mars 2020 mobility system, which has six drive actuators and four steer actuators, will be essentially the same as MSL, with the exception of a set of redesigned and more structurally robust wheels. The MSL-heritage Remote Sensing Mast (RSM), which supports the Mastcam-Z and

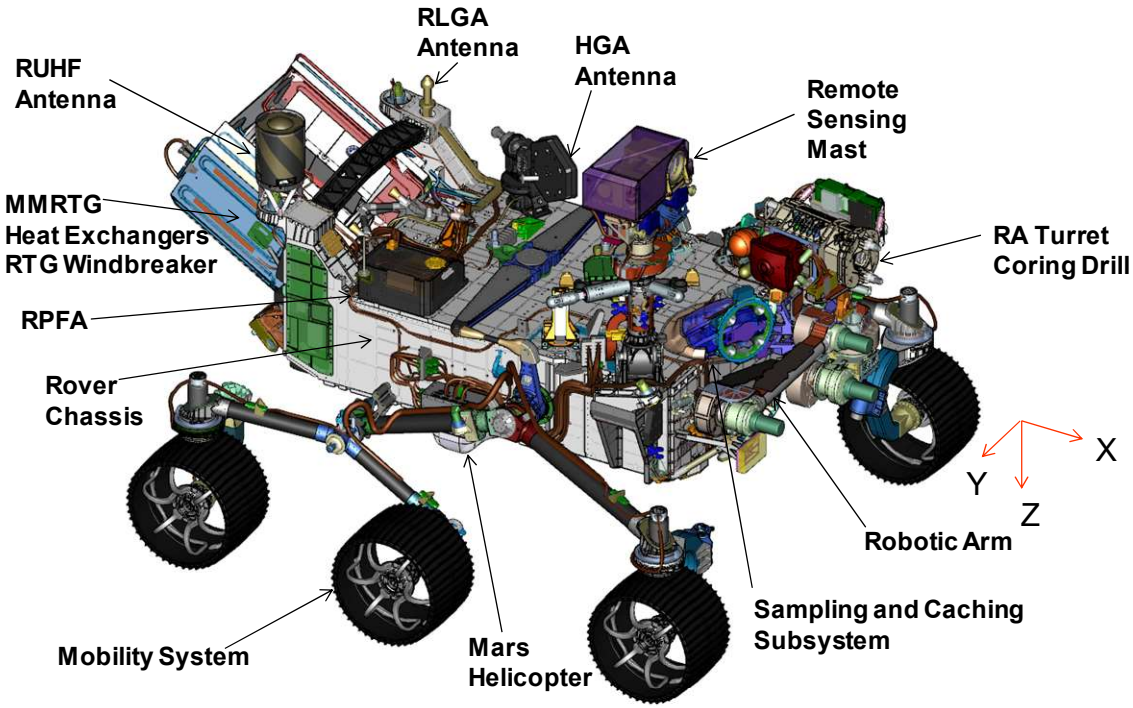

Figure 1. Mars 2020 Rover and External Hardware.

SuperCam science cameras, as well as the engineering Navigation Cameras, stands 2.2 m above the ground. There are three external telecommunications antennas, two operating in the X-band (the RLGA and the HGA) and one in the UHF-band (the RUHF). Direct-to Earth (DTE) communications are done in the X-band and Rover-to-Mars-orbiter communications are done in the UHF-band. The MSL-heritage Rover Pyro Firing Assembly (RPFA) is responsible for firing all Rover launch locks and pyro release devices during Entry Descent and Landing (EDL) and after landing. The Mars 2020 Rover is powered by a radioisotope power system, the MMRTG, which dissipates ~2000W of thermal waste heat. The Mars Helicopter, mounted on the underside of the Rover (on the belly pan), is covered by a debris shield, designed to protect it from sand and pebble strikes during the landing event. The thermal design of the Mars helicopter is described in a previous paper.[3]

II. Description of the Sample Caching Subsystem (SCS) and Sample Handling Assembly (SHA)

There are many other systems on the Mars 2020 Rover that are completely new designs or extensive modifications of hardware that was previously developed for MSL. The Mars 2020 Sampling and Caching Subsystem (SCS), shown in Figure 2, is a completely new subsystem, that resides in the front of the Rover. The SCS is responsible for collecting and caching Mars rock and soil samples in sealed sample tubes and placing them onto the Mars surface. The mission is required to cache 20 returnable samples (16 rock/regolith samples and 4 witness blanks) within the prime mission duration (1.25 Mars years, 836 Sols). These sample tubes will be picked up by a future mission and returned to the Earth. The largest element of the SCS is a five-degree-of-freedom Robotic Arm (RA). A Coring Drill, a Gas Dust Removal Tool (gDRT) and two science instrument sensor heads (PIXL and SHERLOC) are located on the RA turret, at the end of the arm. The Coring Drill, will drill into rocks and soil to collect core samples and store them in sample tubes. These core samples will be transferred into the Adaptive Caching Assembly (ACA) using a Bit Carousel, as shown in Figure 3. The ACA, located under the Rover top deck, houses the Bit Carousel, a Sample Handling Assembly (SHA), a sample tube volume assessment station, a sample tube vision station, a hermetic seal dispenser, a Sealing Station and a drop-off station. The Bit Carousel is used to transfer sample tubes and bits between the inside of the rover (the ACA) and the outside of the rover (the Coring Drill). All of the elements of the ACA are attached to the Caching Component Mounting Deck (CCMD). The CCMD is attached to the rover top deck via three bipods.

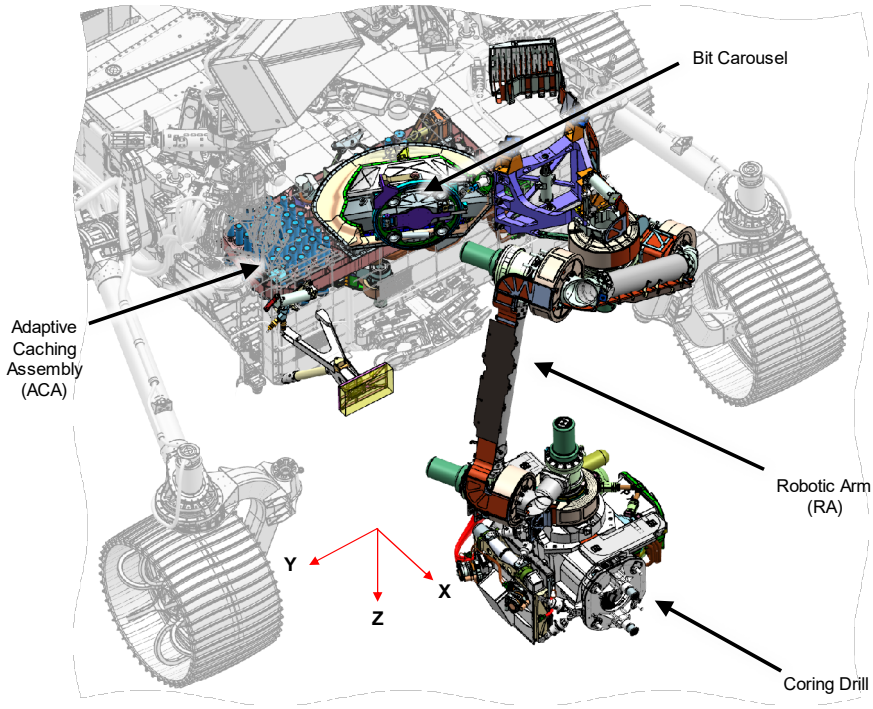

Figure 2. Major Elements of the Sampling and Caching Subsystem (SCS).

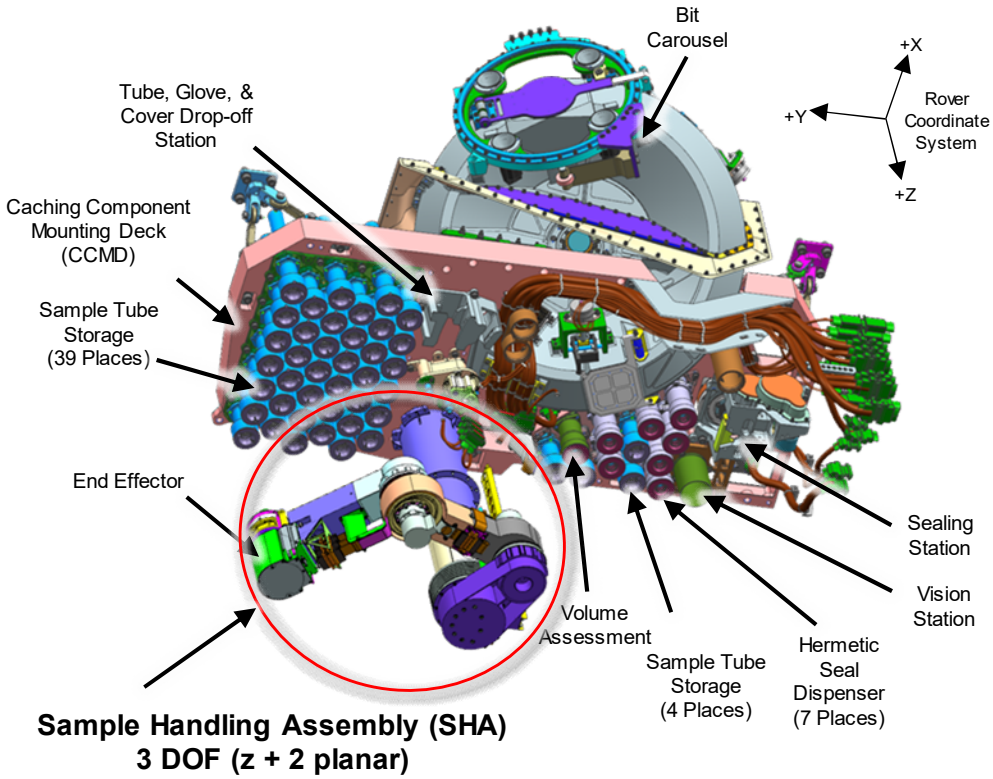

Figure 3. Major Elements of the Adaptive Caching Assembly (ACA) including the Sample Handling Assembly (SHA) and End Effector (EE).

The Sample Handling Assembly (SHA), along with the End Effector (EE), are tasked with moving sample tubes within the ACA. Prior to coring, the SHA will extract an empty sample tube from the sample tube storage and load it into a coring bit. The bit carousel will rotate the bit into position on the outside of the rover, so that the corer can dock with the carousel and exchange the bit to the corer. The RA will place the drill on a soil or rock target and collect a sample. After the sample tube is filled, it will be transferred back into the ACA using the bit carousel. The SHA will extract the filled sample tube out of the bit carousel and move it around to each of the stations within the ACA: the volume assessment station, the vision station, the sealing station, sample tube storage and finally the drop-off station.

Multiple sample tubes will be dropped off in cache depots on the Mars surface for potential future return to Earth. The thermal design of the sample tube is described in an earlier paper.[4] A concept for the Mars sample return is discussed in a previous white paper.[5]

III. SHA & End Effector Thermal Design

The SHA is a 3 degree-of-freedom mechanism using electric-motor-driven actuators to move each of its joints. The End Effector (EE), attached to the free end of the SHA, is designed to grip and release sample tubes and seals that need to be moved within the ACA. All of the SHA and EE mechanisms are wet-lubricated with a Braycote 601EF grease. The viscosity of the grease increases with decreasing temperature; high lubricant viscosity can rob the mechanism of the torque needed to perform its functions. To minimize lubricant viscosity effects and help prevent wear, actuators must be warmed above -55°C and the EE mechanism must be warmed above -25C, prior to operations.

A. Temperature Limits

The SHA and EE have minimum operating and non-operating allowable flight temperature (AFT) limits as shown in Table 1.

Table 1 – SHA & EE Temperature Limits

SHA & End Effector Hardware	Temperature, °C			
	Allowable Flight Limits			
	Operational		Nonoperational	
	min	max	min	max
SHA Linear Stage Mechanism (Slider, Lead Screw, Bearing)	-55	50	-128	50
SHA Linear Actuator (Motor and Gearbox)	-55	50	-128	50
SHA Shoulder Actuator (Motor, Gearbox, and Output Assembly)	-55	50	-128	50
SHA Elbow Actuator (Motor, Gearbox, and Output Assembly)	-55	50	-128	50
SHA End Effector Tube Gripper Actuator (Motor and Gearbox)	-55	50	-128	50
SHA End Effector Gripper Mechanism	-25	50	-128	50
SHA End Effector Force/Torque Sensor	-90	50	-128	50
SHA Flex & Round-wire Harness - across rotating joints	-95	50	-128	50

The minimum operating temperature limit for most SHA components is -55°C. Since the minimum predicted ground temperature at the Holden Crater landing site (environment used for thermal design) is -103°C, there will be times in the mission when the SHA will need to be warmed up, using heaters, above its minimum operating AFT limit, in order to operate. The focus of the SHA thermal design was to locate and size heaters within the mechanism, such that the minimum electrical heater energy could be used to bring the SHA up to its operating

temperature within 3 hours. Originally, the EE Gripper mechanism had a minimum operating temperature limit of -55°C. Later in the design phase, the EE Gripper Mechanism minimum operating temperature limit was increased to -25°C (warmer than the rest of the SHA actuators) to alleviate concerns about mechanism torque margins at colder temperatures. Adjustments to the EE design that were made to accommodate the -25°C minimum operating AFT limit are discussed later in this paper. Unheated hardware in the SHA and EE, the EE force/torque sensor and the flex and round-wire harness have minimum operating temperature limits of -90°C and -95°C, respectively. All non-operating temperature limits are -128°C to 50°C. The maximum operating temperature limit for the actuators (50°C) refers to the maximum "turn-on" temperature of the actuator. Actuators are allowed to self-heat above 50°C due to motor power dissipation. Internal motor components (e.g., motor windings, brake windings, Hall effect sensors, etc.) are protected by on-board fault protection software. The fault protection software uses test-correlated thermal models to predict internal motor temperatures and will turn off the motors if internal temperatures are predicted to exceed allowable limits.

B. Thermal Model Description

Figure 4 shows a comparison of the SHA and EE thermal and solid models. The Thermal Desktop® (TD) analytical thermal model of the SHA & EE has 2181 elements and 6532 nodes. Since the SHA is enclosed inside the ACA, it does not see a direct solar load when it is operating on Mars. In order to minimize the radiation heat loss from the SHA, when the warm-up heaters are operating, most of the mechanism surface coatings were low emissivity (bare metal or Tiodize Type II). The ACA has a deployable belly pan that allows the shoulder, elbow and end effector to be exposed to the Mars atmosphere below the belly pan, when the linear stage is fully extended. The deployable belly pan is a design feature of the ACA that allows maximum extension of the SHA and provides a vent path for potential outgassing and contamination from the ACA to the Mars environment.

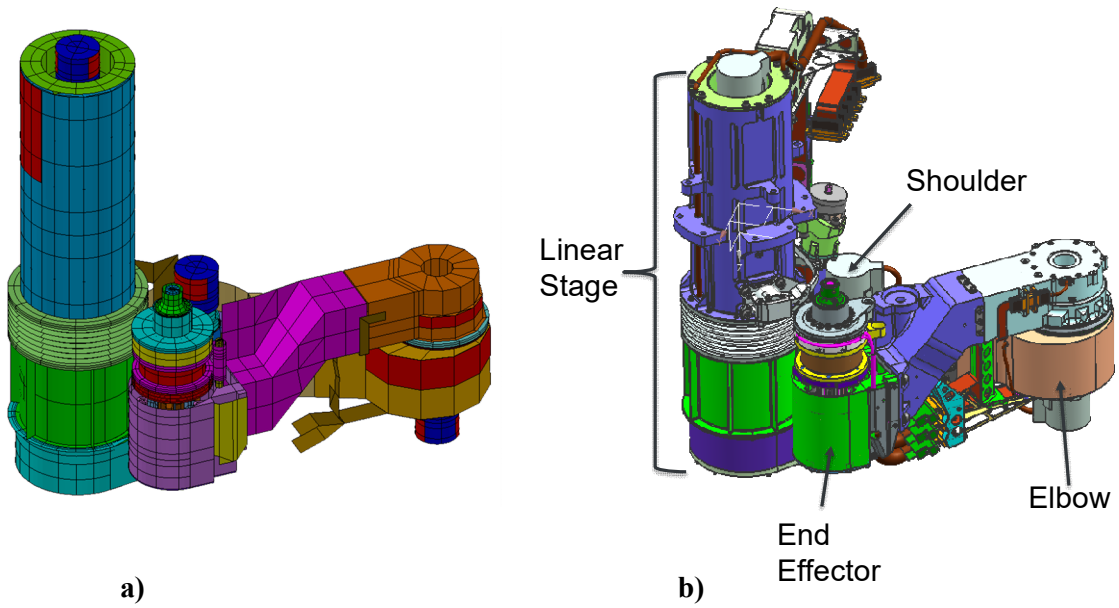

Figure 4. SHA & EE Stowed Configuration – a) Thermal Desktop® Model and b) Solid Model.

C. Heater and Temperature Sensor Locations

Heaters and temperature sensors (used for heater control, fault protection and heater performance information) were located as close as possible to hardware that needed to be warmed above -55°C prior to operation. Figures 5a, 6a and 7a show all of the hardware locations (colored in red) that needed to be warmed up to -55°C prior to operations. All of the SHA hardware elements needing warm-up heat have single string warm-up heaters and redundant Platinum Resistance Thermometers (PRTs) to control those heaters. The heaters have cross-strapped power switches (and redundancy at the Rover switch level), but a limitation on the number of flex cable traces available for heaters led to a decision to accept single-string heater elements. Temperature sensors are used for heater control feedback, for fault monitoring (to protect against a motor overheat condition) and for information about mechanism heating performance.

Figure 5b shows the locations of the 8 heaters and 6 PRTs on the Linear Stage. Two heaters running down the full length of the slide adaptor and 4 heaters at the top and bottom of the external housing were designed to help warm up the rollers and the lead screw that runs down the middle of the slide adaptor. Two PRTs near the +Z external housing heaters are used to control all of the heaters in the linear stage heater zone. A heater and two "information-only" PRTs were added to the lead screw nut to aid in understanding how the lubricant, in the interface between the nut and the lead screw, is warmed up. The Linear stage gear-motor was also equipped with a heater and two fault protection monitor PRTs (designed to prevent motor overheat).

An onboard transient thermal model (resident in the Rover's flight software) is used to predict the temperature of the motor windings of all four SHA/EE motors. Fault protection will shut down the motors if a maximum motor winding temperature limit (130°C) is predicted to be exceeded. A real-time, motor housing temperature, measured by the motor PRT, is used by flight software to update the fault protection thermal model. Note that there are no PRTs mounted directly on the EE motor housing. There is still fault protection running in flight software for this motor, it just uses a slightly modified thermal model that is seeded with an initial temperature based on the reading from the EE PRT mounted on the Tube Gripper angular plate, below the lower housing heater (see Figure 7b).

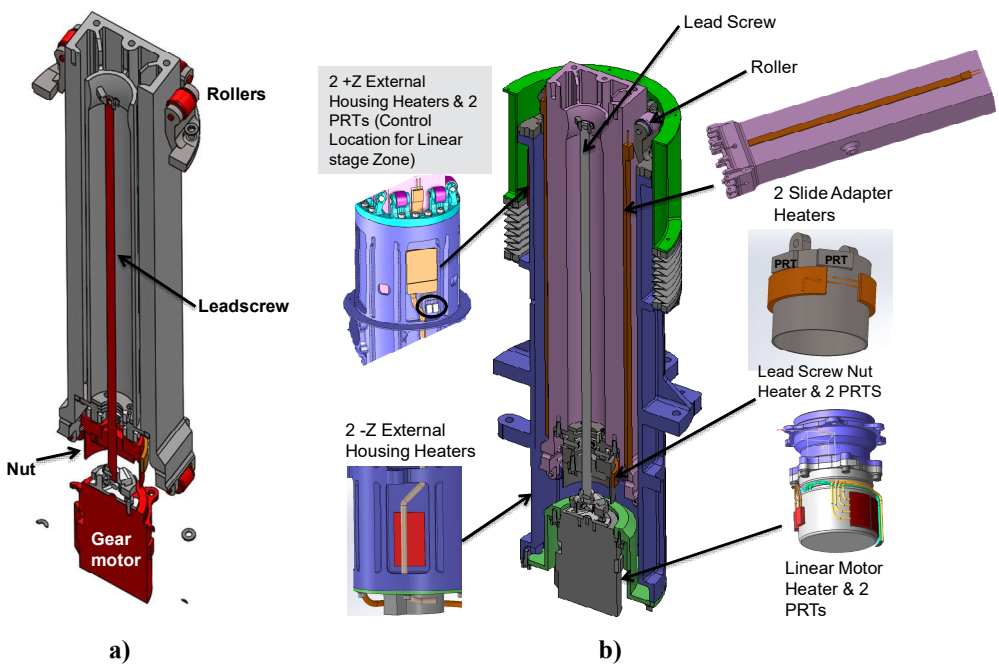

Figure 5. Linear Stage – a) Locations of Hardware that needs preheat shown in red, b) Locations of Heaters and PRTs.

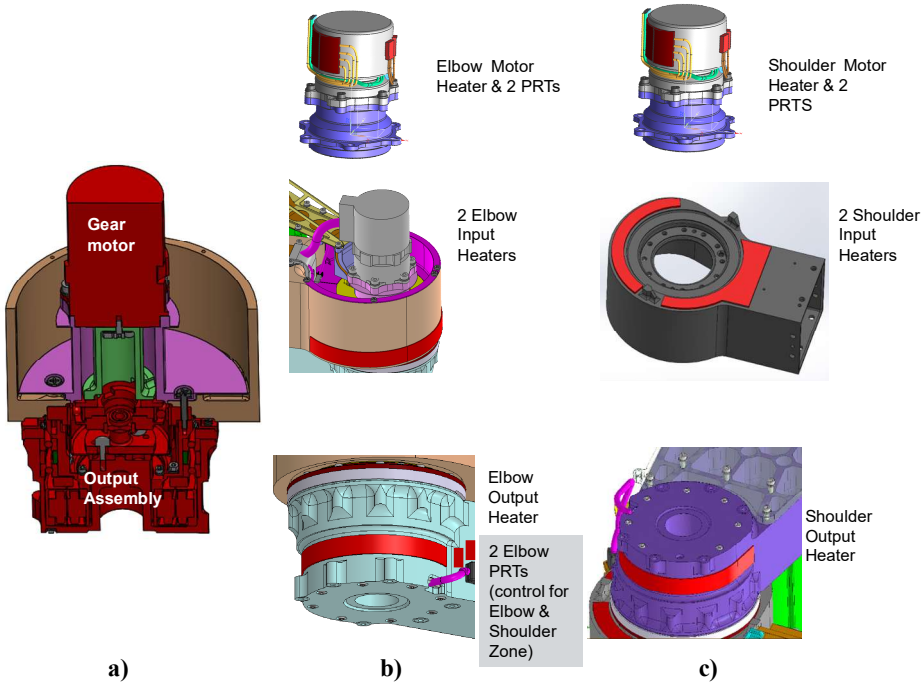

Figure 6. Elbow & Shoulder Actuators - a) Locations of Hardware that needs preheat shown in red b) Elbow Actuator: Locations of Heaters and PRTs, c) Shoulder Actuator: Locations of Heaters and PRTs

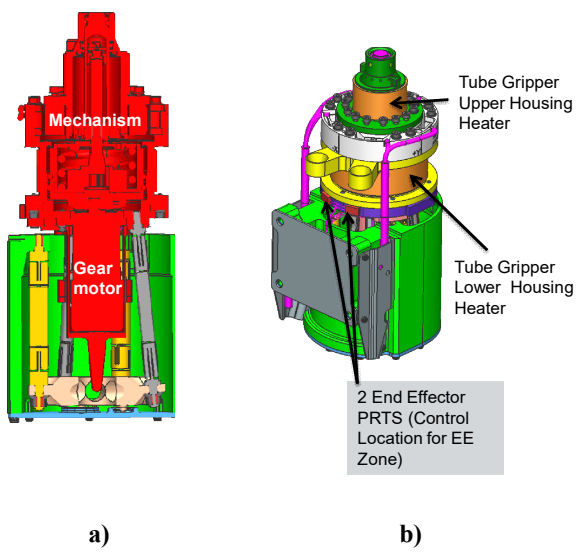

Figure 7. EE – a) a) Locations of Hardware that needs preheat shown in red, b) Locations of Heaters and PRTs.

Figures 6b and 6c show the locations of the 8 heaters and 6 PRTs on the elbow and shoulder actuators. Heaters are located on the motors, input gearboxes and output gearboxes of each actuated joint. The shoulder & elbow heater zone is controlled by the 2 PRTs on the Elbow Actuator output gearbox. The 4 PRTs on the shoulder and elbow motors are used for fault protection monitoring.

Figure 7b shows the locations of the 2 heaters and 2 PRTs on the EE. Heaters on the upper and lower housing of the EE warm the tube gripper mechanism and tube gripper gear-motor. It was not possible to put heaters or PRTs directly on the tube gripper gear-motor, since that portion of the mechanism is mounted on flexures and must be able to move freely inside the tube gripper housing. The EE heater zone is controlled by the 2 PRTs mounted below the tube gripper lower housing heater, on the end effector angular plate.

In summary, there are 8 heater elements on the linear stage dissipating 26W (at 28V), 8 heater elements on the Shoulder and Elbow actuators and outputs dissipating 53W (at 28V) and two heaters on the EE dissipating 8.85W (at 28V). Heater sizing was done over a bus voltage range of 28V to 32.8V. Thus, there are 3 distinct SHA/EE heater zones: 1) Linear Stage, 2) Shoulder & Elbow and 3) EE. Heater elements in a single zone are wired up in parallel. There are 14 PRTs on the SHA and EE, 6 of which are used for heater control. Guidelines for sizing and design of heaters on gear-motor actuators are presented in a previous papers.[6-8]

IV. Thermal Design Assumptions & Requirements

When this thermal design and analysis was completed, the final Mars 2020 landing site (Jezero Crater) had not yet been selected. At the time, there were still 8 candidate landing sites being considered, over a latitude range of 26.4 deg South to 24 deg North. Due to the eccentricity of the Mars orbit and the planet's axis tilt, the southern hemisphere landing sites have hotter summers (Mars is closer to the Sun at Summer Solstice in the southern hemisphere) and colder winters (Mars is farther from the Sun at Winter Solstice in the southern hemisphere). Of these 8 sites, the most southerly site, Holden Crater (26.4 deg S latitude), imposed the most extreme thermal environments, so it was chosen to be the worst-case landing site for the thermal design of the SHA and EE. Worst-case Hot (Summer) and Cold (Winter) thermal design environments for Holden Crater are shown in Figure 8. Papers describing the Mars Weather Research and Forecasting Model (Mars WRF) simulation software, used to generate these environments, have been published previously.[9-11] Sustained freestream wind speeds at the landing site were assumed to range from 0 m/s to 15 m/s.

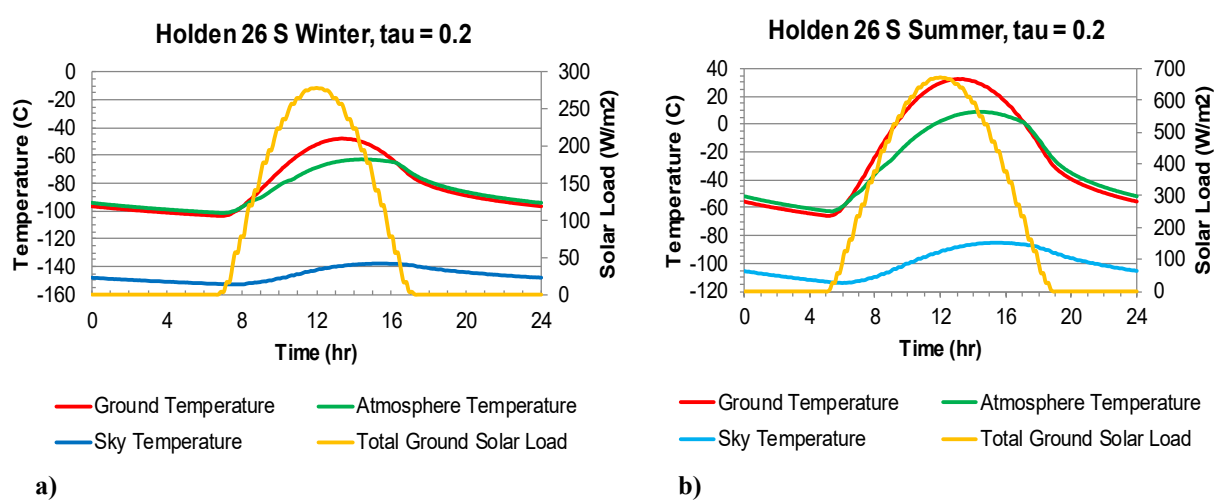

Figure 8. Worst-Case Cold & Hot Design Environments in Holden Crater – a) Winter (Ls = 91 degrees) & b) Summer (Ls = 259 degrees).

The final selection of Jezero Crater (18.5 deg N latitude) as the Mars 2020 landing site was good news for the SHA thermal design, which had been done for the more stressful landing site environment at Holden Crater and will have plenty of thermal margin in the more benign environment at Jezero Crater. Comparisons between maximum and

minimum ground temperatures over the entire Martian year, in the Holden (thermal design) and Jezero (flight) environments, are shown in Figure 9 below. The Jezero flight environments are more benign (i.e., warmer in the cold case and cooler in the hot case) than the Holden design environments. The Jezero cold case has a minimum ground temperature (-90°C) that is 13°C warmer than the minimum ground temperature at Holden Crater (-103°C). The Jezero hot case has a maximum ground temperature (14°C) that is 18°C cooler than the maximum ground temperature at Holden Crater (32°C). The minimum ground temperature at the Jezero landing site occurs at Ls = 281 degrees, near Winter Solstice (Ls=270 degrees) in the Northern Hemisphere. However, the maximum ground temperature at the Jezero landing site occurs at Ls = 179 degrees, near Fall Equinox (Ls=180 degrees) in the Northern Hemisphere.

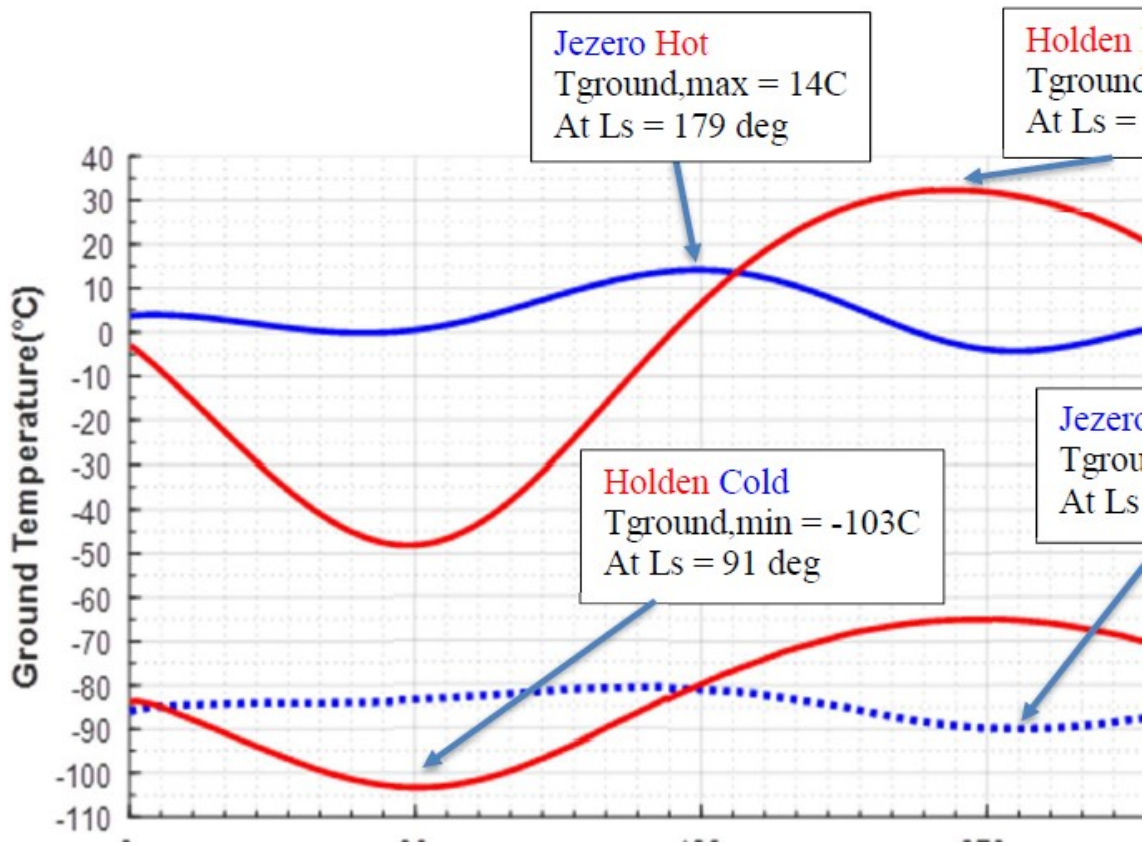

Figure 9. Comparison of Maximum and Minimum Ground Temperatures over the Entire Martian Year in the Holden (design) and Jezero (flight) Landing Site Environments

There is a Design Principle (DP) requirement to keep the predicted duty cycles of thermostatically-controlled heaters to less than 80% (thus oversizing the heaters to maintain 20% of duty cycle margin). Heaters were sized for a bus voltage range of 28V to 32.8V. There are no requirements specific to warm-up heater energy consumption, but in general there is a desire to minimize heater energy consumption to allow more energy to be used for science, avionics and mobility.

V. Thermal Model Predictions

The Rover system-level thermal model was used to generate diurnal boundary conditions for the ACA cavity (where the SHA is located inside the Rover) in the Worst-Case Cold (WCC) and Worst-Case Hot (WCH) environments. The SHA thermal model (see Figure 4a) was first run in the "soak" condition (no internal dissipation inside the ACA) for the cold case with no wind. Temperature predictions for that case are shown in the plot of Figure 10. In the WCC environment (with 0 m/s wind), none of the actuators are naturally warmed up by the

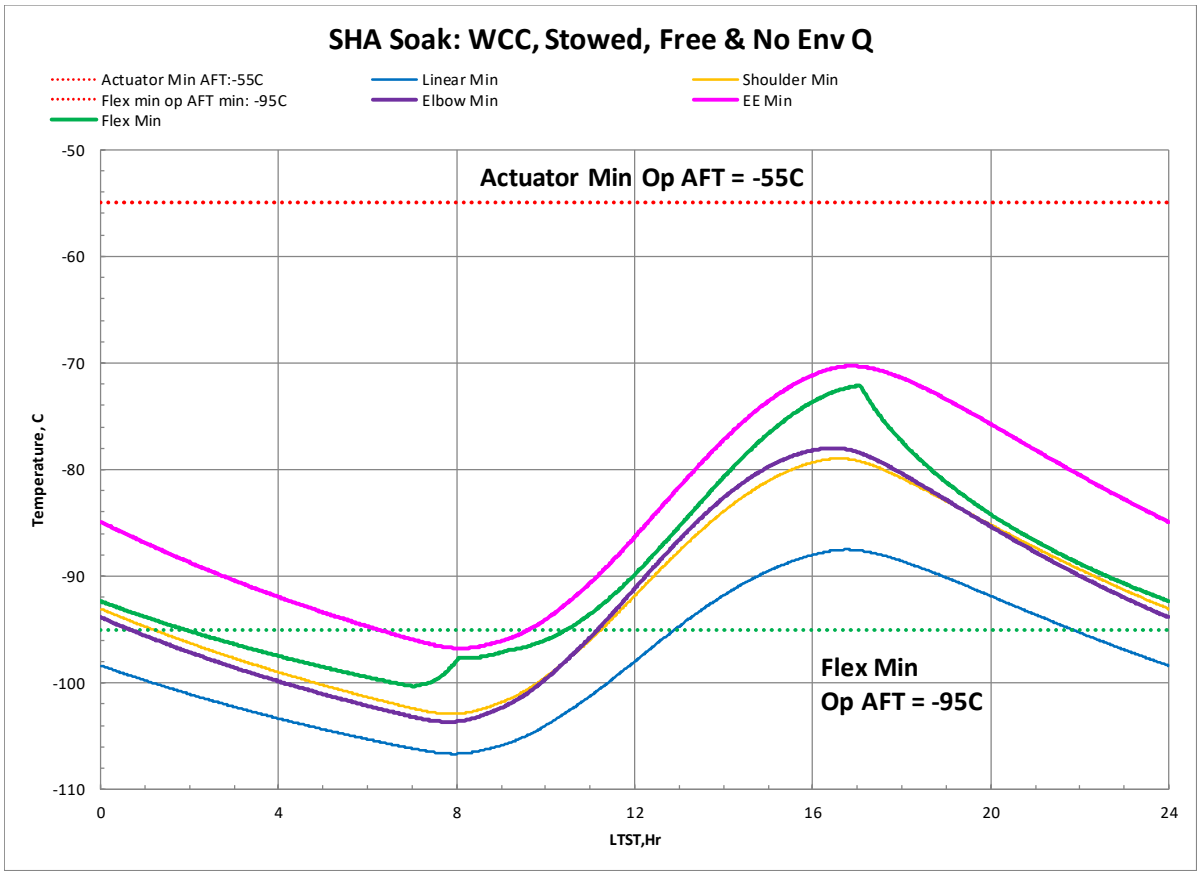

Figure 10. Predicted Diurnal Soak Temperatures for all SHA & EE actuators and Flex Cable in the Holden Crater Worst-Case Cold Winter Environment (no wind).

environment above the minimum operating AFT limit of -55°C. All actuators remain below -70°C for the entire Sol, still 15°C below their minimum operating AFT limits of -55°C. Clearly there is a need for warm-up heaters to bring the actuators up to operating temperatures.

Heaters were sized and placed within the SHA thermal model as described in Section III of this paper. Then the model was run in the WCC environment with 15 m/s wind. Results of a warm-up simulation in the WCC environment with 15 m/s wind are shown in Figure 11. The heaters are turned on at 0800 LTST (the earliest desired warmup start time) and warm the SHA & EE up to operating temperature within 3 hours. The 3-hour warm-up uses 260 W*hr of energy. All heated elements are above -55°C by 1100 LTST. The minimum temperatures of hardware within the three heating zones (Linear Stage, Shoulder/Elbow & EE) all rise to -55°C at about the same time, indicating that the heaters are well balanced across the zones. After 1100 LTST, the heater operation transitions into a thermostatically-controlled maintenance mode, with all duty cycles of 79% or less. This meets the Design Principle requirement stipulating that heater design duty cycles must be less than 80%. The SHA flex cable is also well above its minimum operating temperature limit of -95°C, by 1100 LTST. The model results shown in Figure 11 are for a stowed SHA, inside the ACA. Another warm-up heater run was done for a fully-extended SHA (shoulder, elbow and EE below the belly pan) and it was found that the warm-up duration was only extended by 9 minutes. The warm-up heater design is not sensitive to SHA configuration (stowed vs. fully-extended).

This analysis assumed an EE minimum operating AFT limit of -55C. Later in the design phase, the EE minimum operating AFT was changed to -25C. Concerns about low torque margins and excessive drag in the EE mechanism, discovered when it was tested at cold temperatures, necessitated the temperature limit change. As a result, the EE tube gripper lower housing heater size was increased from 5W to 7W. Warm-up energy (for the 0800 LTST warm-

up) increased from 15 W*hr to 33 W*hr, a significant, but still acceptable increase. The predicted heater duty cycle increased from 63% to 78%, still below the 80% maximum allowable duty cycle limit.

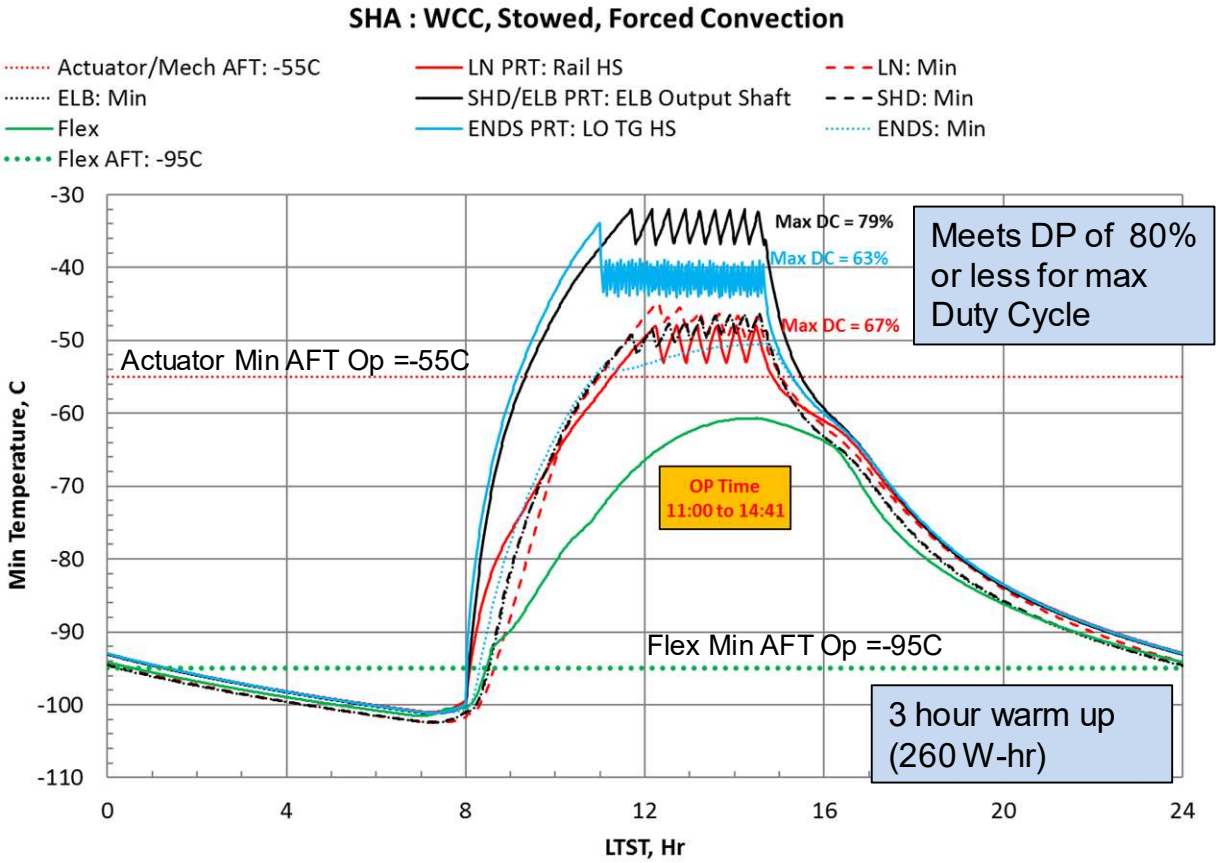

Figure 11. Predicted Temperatures for all SHA & EE actuators and Flex in the Holden Crater Worst-Case Cold Winter Environment (15 m/s wind) with an 0800 LTST warm-up start time.

Figure 12 shows the results of a hot case diurnal soak analysis run. In the WCH environment (with no wind), there is a rather sizeable "no-heat" window for operating the SHA and EE. Between the hours of 1105 and 2122 LTST (for approximately 10 hours), the SHA and EE hardware are naturally warmed up, by the environment, above the minimum operating AFT limit of -55°C. The Linear Stage components are the last to warm up, mainly because they are layered inside an external housing and are not as well-coupled to the environment as the EE and Shoulder/Elbow hardware. If 15 m/s wind is added into the WCH environment, the no-heat window widens to 0904 to 2354 LTST (approximately 15 hours long).

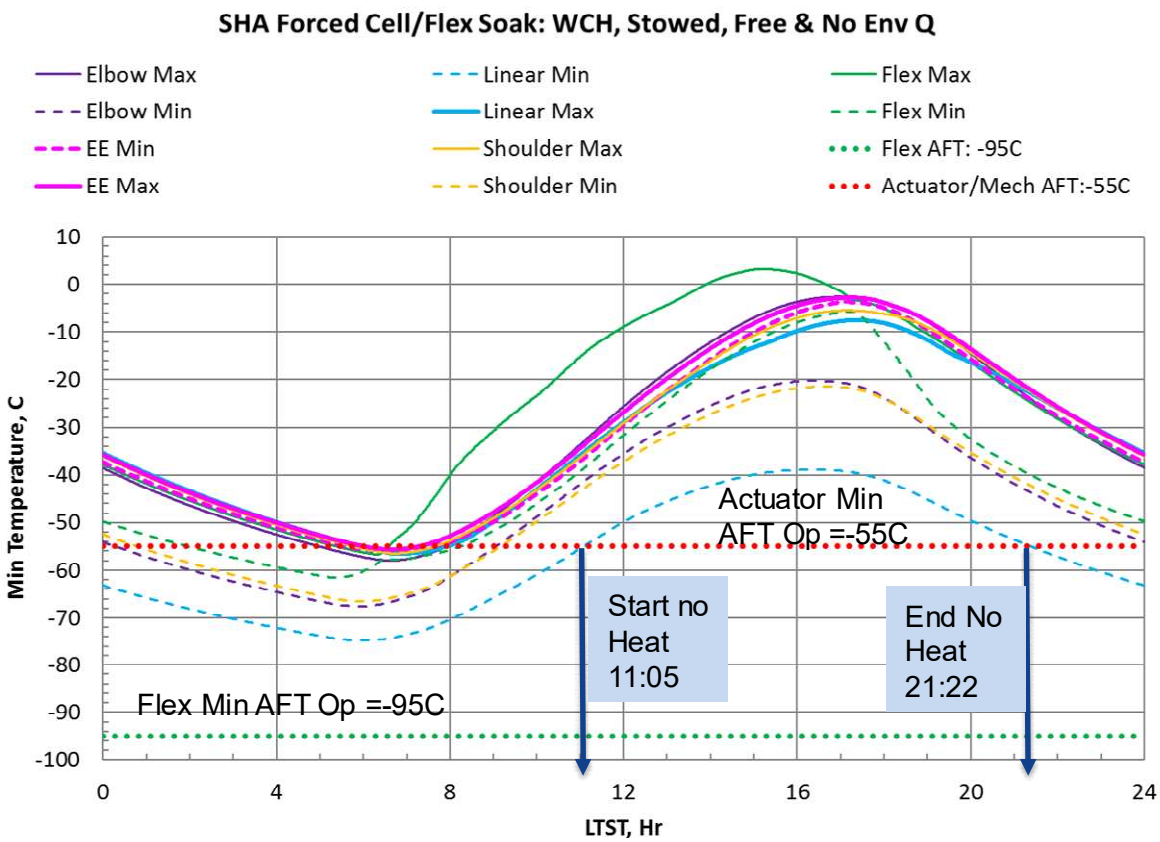

Figure 12. Predicted Diurnal Soak Temperatures for all SHA & EE actuators and Flex in the Holden Crater Worst-Case Hot Summer Environment.

The last thermal design issue that needed to be analyzed with the SHA model was a hot operating case. Figure 13 shows the motor winding temperatures of the three higher power dissipation motors in the SHA, during operations in the WCH environment, with wind. Forced convection was the driving hot case for motor operations because it results in the warmest initial turn on temperature for the motors. Conservative (biased hot) power levels and durations were assumed for all three motors. The Linear actuator motor was assumed to dissipate 2.5W over 3.5 hours, while the Shoulder and Elbow motors dissipated a nominal power of 0.75W for 2.5 hours and a peak power of 1.5W for 1 hour. EE motor power dissipation was not modeled because its power level is low and the duty cycle is also very low. The highest power motor, the linear stage, reaches a peak, steady-state motor winding temperature of 75°C, still 55°C below the maximum allowable winding temperature of 130°C. Clearly, there is plenty of margin against motor overheat. A free convection, hot operating case was also run, which resulted in cooler initial motor winding temperatures and cooler motor winding peak temperatures during operations.

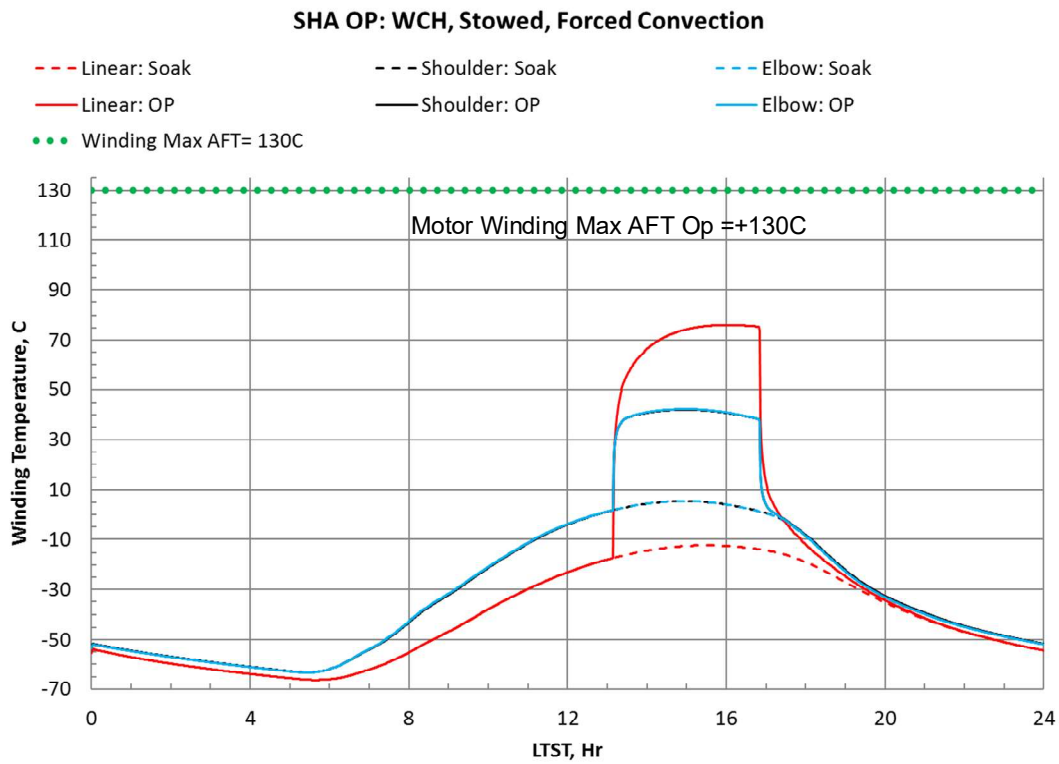

Figure 13. Predicted Motor Winding Temperatures for all SHA Actuators in the Holden Crater Worst-Case Hot Summer Environment with a 1300 LTST operating start time.

VI. Future Thermal Testing of the SHA and EE

Thermal testing of the SHA & EE, after it has been integrated into the entire ACA, is planned to start in June of 2019. At that time, all of the CCMD-mounted components will be put inside a thermal chamber and cycled over the non-operating qualification temperature range of -135°C to +70°C. In addition, the ACA hardware will see a planetary protection bakeout at 110°C. The SHA will be fully instrumented with thermocouples. A simple thermal characterization test will be done on the SHA & EE that entails turning on the heaters, with the chamber and hardware soaked at -110°C, and allowing the hardware to warm up to steady state. After a thermal steady-state condition has been reached, the heaters will be turned off and the hardware will be allowed to cool. This test case will allow a thermal engineer to correlate the thermal model of the SHA & EE. The steady state condition at peak temperatures will allow adjustments to be made to the model resistance network. Once that is completed, the distributed thermal capacitances in the model can be adjusted to correlate to the transient test data collected during the warm-up and cooldown. Additional functional operating test cases will be done with the hardware soaked to -70°C (the minimum operating qualification temperature limit) and with the hardware warmed up from -110°C to -70°C using the warm-up heaters. Once this testing is completed, the SHA & EE will be qualified for flight and the thermal model can be correlated and updated based on the test data. The correlated model will be used to develop heating prescriptions for SHA & EE hardware that can be used during surface operations in Jezero Crater. A previous paper describes how heating table prescriptions will generated and used in Mars 2020 surface operations.[12]

VII. Conclusion

A robust thermal design for the SHA and EE has been completed. The design is based on a worst-case environment for Holden Crater. The Mars 2020 mission has selected Jezero Crater as its official landing site. Jezero Crater has a more benign environment (cooler in the hot case and warmer in the cold case) than Holden Crater. Thus the thermal design described in this paper will perform even better (with larger margins) during Mars 2020 surface operations.

Acknowledgments

This work was conducted at the Jet Propulsion Laboratory, California Institute of Technology, under a contract with the National Aeronautics and Space Administration. We would like to thank Milo Silverman (ACA Cognizant Engineer), Brad Kobeissi (SHA Cognizant Engineer at JPL) and Andrew Bertolucci (SHA Mechanical Design Engineer at SSL-MDA) for their support in a number of discussions related to the thermal design and thermal hardware accommodation within the SHA mechanical design. Without their inputs, this work would not have been possible.

References

[1] Novak, K., Kempenaar, J., Redmond, M., and Bhandari, P., "Preliminary Surface Thermal Design of the Mars 2020 Rover," ICES 2015-134, 45th International Conference on Environmental Systems, Bellevue, WA, July 2015.

[2] Kempenaar, J., Novak, K. , Redmond, R., Farias, E., Singh, K., and Wagner, M., "Detailed Surface Thermal Design of the Mars 2020 Rover," ICES 2018-53, 48th International Conference on Environmental Systems, Albuquerque, NM, July 2018.

[3] Schmidt, T., Cappucci, S., Miller, J., Wagner, M., Bhandari, P., and Pauken, M., "Thermal Design of a Mars Helicopter Technology Demonstration Concept," ICES-2018-018, 48th International Conference on Environmental Systems, Albuquerque, NM, July 2018.

[4] Redmond, M., Sherman, S., Bhandari, P., & Novak, K., "Thermal Design, Analysis, and Sensitivity of a Sample Tube on the Martian Surface," 47th International Conference on Environmental Systems, Charleston, SC, July 16-20, 2017.

[5] iMARS Working Group (2008), "Preliminary Planning for an International Mars Sample Return Mission", available at https://mepag.jpl.nasa.gov/reports/iMARS_FinalReport.pdf

[6] Novak, K., Liu, Y., Lee, C-J., and Hendricks, S., "Mars Science Laboratory Rover Actuator Thermal Design," 40th International Conference on Environmental Systems, Barcelona, Spain, July 11-15, 2010.

[7] Redmond, M., Novak, K., Mireles, V., "Static Ball Bearing Thermal Conductance in Air and Vacuum: Review and Correlation," AIAA Journal of Thermophysics and Heat Transfer, Vol. 31, No. 4, 2017, pp. 841-846.

[8] Redmond, M., Kempenaar, J., and Novak, K., "Mars 2020 Mobility Actuator Thermal Testing and Model Correlation," 47th International Conference on Environmental Systems, Charleston, SC, July 16-20, 2017.

[9] Richardson, M.I., Toigo, A.D., Newman, C.E., 2007. "PlanetWRF: a general purpose, local to global numerical model for planetary atmospheric and climate dynamics", J. Geophys. Res. 112, E09001. http://dx.doi.org/10.1020/2006JE002825.

[10] Toigo, A.D., Lee, C., Newman, C.E., Richardson, M.I., 2012. "The impact of resolution on the dynamics of the martian global atmosphere: varying resolution studies with the MarsWRF GCM.", Icarus 221, 276–288.

[11] Mischna, M.A., Lee, C., Richardson, M., 2012. "Development of a fast, accurate radiative transfer model for the Martian atmosphere, past and present", J. Geophys. Res. 117, E10009. http://dx.doi.org/10.1029/2012JE004110.

[12] Novak, K., Redmond, M., Kempenaar, J., Farias, E., and Singh, K., "Thermal Operability Improvements for the Mars 2020 Rover Surface Mission," ICES 2018-13, 48th International Conference on Environmental Systems, Albuquerque, NM, July 2018.